In Vivo Chondrogenesis in 3D Bioprinted Human Cell-laden Hydrogel Constructs

OPEN

PRS GLOBAL OPEN EXPERIMENTAL

In Vivo Chondrogenesis in 3D Bioprinted Human Cell-laden Hydrogel Constructs

Thomas Möller, MSc*
Matteo Amoroso, MD†
Daniel Hägg, PhD*
Camilla Brantsing, MSc‡
Nicole Rotter, PhD§
Peter Apelgren, MD†
Anders Lindahl, PhD‡
Lars Kölby, PhD†
Paul Gatenholm, PhD*

Background: The three-dimensional (3D) bioprinting technology allows creation of 3D constructs in a layer-by-layer fashion utilizing biologically relevant materials such as biopolymers and cells. The aim of this study is to investigate the use of 3D bioprinting in a clinically relevant setting to evaluate the potential of this technique for in vivo chondrogenesis.
Methods: Thirty-six nude mice (Balb-C, female) received a 5- × 5- × 1-mm piece of bioprinted cell-laden nanofibrillated cellulose/alginate construct in a subcutaneous pocket. Four groups of printed constructs were used: (1) human (male) nasal chondrocytes (hNCs), (2) human (female) bone marrow–derived mesenchymal stem cells (hBMSCs), (3) coculture of hNCs and hBMSCs in a 20/80 ratio, and (4) Cell-free scaffolds (blank). After 14, 30, and 60 days, the scaffolds were harvested for histological, immunohistochemical, and mechanical analysis.
Results: The constructs had good mechanical properties and keep their structural integrity after 60 days of implantation. For both the hNC constructs and the cocultured constructs, a gradual increase of glycosaminoglycan production and hNC proliferation was observed. However, the cocultured group showed a more pronounced cell proliferation and enhanced deposition of human collagen II demonstrated by immunohistochemical analysis.
Conclusions: In vivo chondrogenesis in a 3D bioprinted human cell-laden hydrogel construct has been demonstrated. The trophic role of the hBMSCs in stimulating hNC proliferation and matrix deposition in the coculture group suggests the potential of 3D bioprinting of human cartilage for future application in reconstructive surgery. *(Plast Reconstr Surg Glob Open 2017;5:e1227; doi: 10.1097/GOX.0000000000001227; Published online 15 February 2017.)*

Cartilage is an avascular tissue that once degenerated or wounded has limited ability to heal. Current reconstructive options for cartilage repair[1] or replacement[2] are limited by numerous problems and the lack of suitable cartilage substitute poses a major challenge. The demand for cartilage tissue restoration is therefore high. Three-dimensional (3D) bioprinting technology may represent a possible solution.

The bioprinting technology can generate 3D tissue through the precise deposition of cells and supporting structures simultaneously, in a layer-by-layer fashion.[3–6] In cartilage 3D printing, ink-jet printing[7] and extrusion printing[8] are the most commonly used techniques. Hydrogels represent the main material used as bio ink.[9] Hydrogels can be synthetic like polyethylene glycol

*From the *3D Bioprinting Centre, Department of Chemistry and Chemical Engineering, Chalmers University of Technology, Göteborg, Sweden; †Gothenburg University, Sahlgrenska Academy, Institute of Clinical Sciences, Department of Plastic Surgery, Sahlgrenska University Hospital, Göteborg, Sweden; ‡Department of Clinical Chemistry and Transfusion Medicine, Institute of Biomedicine, Sahlgrenska University Hospital, Göteborg, Sweden; and §University Medical Center Ulm, Department of Otorhinolaryngology, Frauensteige 12, 89075 Ulm, Germany.*
Received for publication November 16, 2016; accepted December 19, 2016.
Presented at (1) "13th Congress of the European Federation of Societies for Microsurgery." Oral presentation title: "In vivo chondrogenesis in 3D-bioprinted human chondrocyte-laden hydrogel constructs," April 2016, Antalya, Turkey; (2) "The 36th Congress of the Scandinavian Association of Plastic Surgeons." Oral presentation title: "In vivo chondrogenesis in 3D-bioprinted human chondrocyte-laden hydrogel constructs," June 2016, Uppsala, Sweden; and (3) "Kirurgvekan 2016." Oral presentation title: "In vivo chondrogenesis in 3D-bioprinted human chondrocyte-laden hydrogel constructs," 2016, Malmö, Sweden.

DOI: 10.1097/GOX.0000000000001227

Disclosure: *The authors have no financial interest to declare in relation to the content of this article. The Article Processing Charge was paid for by the authors.*

based[10] on natural polymers like collagen,[11] hyaluronic acid[12] chitosan,[13] or alginate,[14] and are used because of their high biocompatibility and low cytotoxicity. Their high water content gives them a structural similarity to extracellular matrix (ECM) of cartilage.[9,15] One of the shortcomings of hydrogels is their viscoelastic properties, which hamper good printing fidelity (fine line resolution). Another problem is their mechanical properties, such as strength and stiffness, which make them difficult to handle during transplantation. An additional requirement for an ideal bionic for in vivo use is long-term structural stability. To compensate the inability of hydrogel to maintain a uniform 3D structure, a supporting polymer[16] or combination with other materials such as gelatin[17] can be used. We have recently showed that all these shortcomings can be overcome by formulating a bioink based on nanofibrillated cellulose and alginate.[18] Although substantial progress has been made, the lack of mechanical and structural integrity of the 3D constructs still represents a major challenge. The inability of the scaffold to keep its 3D shape and tolerate load-bearing has limited the application in vivo of the 3D printed tissues, such as cartilage. The recently developed a novel bioink has proved to be able to generate constructs with stable architecture and adequate mechanical properties. This new bionic combines the shear thinning properties of nanofibrillated cellulose (NFC) with the fast cross-linking ability of alginate. It can therefore be considered a promising hydrogel for 3D bioprinting with living cells for growth of cartilage tissue.[18] Attempts to generate cartilage structures have been largely based on chondrocytes[19] and mesenchymal stem cells (MSCs) used individually.[20] However, the combination of both cell sources in mixed cell cultures has been demonstrated to enhance chondrogenesis.[21,22] In this study, we aimed to investigate the use of 3D bioprinting in a clinically relevant setting to evaluate the potential of this technique for in vivo chondrogenesis.

MATERIALS AND METHODS

Cell Types and Cell Culture

Human bone marrow–derived stem cells (hBMSCs) originally derived from a female donor (Rooster Bio, MD) and human nasal chondrocytes (hNCs) originated from a male donor undergoing septum rhinoplasty at the Department of Otorhinolaryngology of Ulm, University Medical Centre (ULM, Germany, Ethical permission no. 152/08) were used. The hBMSCs were cultured under standard culture conditions (37°C, 5% CO_2, humidified) using an hBM-MSC High Performance Media Kit (Rooster Bio). The hBMSCs were passaged once after 4 days in culture and harvested for printing on day 8. The hNCs were cultured for 6 days in DMEM/F-12 medium (Life Technologies, Waltham, MA) supplemented with 10% fetal bovine serum (HyClone, GE Healthcare, South Logan, UT) and 1% penicillin/streptomycin (HyClone, GE Healthcare) without additional passages, and then harvested for printing.

3D Bioprinting of Gridded Structures

A nanofibrillated cellulose/alginate (NFC-A) bioink (CELLINK AB, Gothenburg, Sweden) was used for printing lattice-shaped constructs using a pneumatic extrusion bioprinter INKREDIBLE (CELLINK AB) mounted in a LAF bench. For homogenous mix of the cells with the NFC-A bioink in a ratio of 1:11, a cell mixer was used (CELLINK AB).

The initial cell density for all groups was 10×10^6 cells/ml bioink. After printing, the lattice structured grids were cross-linked with 100 mM $CaCl_2$ solution for 5 minutes at 37°C. Thereafter, cell-free structures were washed with Hanks balanced salt solution (HyClone, GE Healthcare) supplemented with 5 mM $CaCl_2$, whereas cell-laden constructs were washed with their respective cell culture medium at 37°C. Printed constructs were implanted into nude mice within 1 hour after printing. For day 0, cell-laden constructs were simulated by mixing DMEM/F-12 medium (Life Technologies), instead of cell suspension, with the bioink. Mixing ratio was the same as for cell-laden constructs.

Subcutaneous Implantation of Scaffolds in Mice and Experimental Groups

To evaluate neocartilage formation and the stability of the bioprinted constructs in vivo, cell-laden and cell-free constructs were implanted subcutaneously on the back of 6-week-old nude female mice (Balb-C, 9 animals per group). Wounds were sutured with 6.0 Vicryl Rapid (Ethicon, Sommerville, NJ) and covered with a sterile wound tape. The animal experiments were approved by the Ethical committee for experimental animals, University of Gothenburg (No. 119-2015). Four different experimental groups were implanted: (1) cell-free scaffolds; (2) scaffolds with hNCs; (3) scaffolds with hBMSCs; and (4) scaffolds with a coculture of hNCs and hBMSCs (20%/80%). Mice were anesthetized using an intraperitoneal injection of Ketamin (50 mg/ml) and Dormitor (1 mg/ml), mixed in a 1:1 ratio. The injection dose was 0.05 ml per 20 g animal weight.

Over the implantation period, the overall behavior and wound healing were assessed by visual inspection. After 14, 30, and 60 days, 3 animals per group were terminated and the construct was explanted. From each construct, one-third was used for mechanical analysis and the other two-thirds were used for histological and immunohistochemical analyses.

Histological Analysis

To qualitatively evaluate the formation of neocartilage, the constructs were harvested after 14, 30, and 60 days of subcutaneous implantation.

Explants were fixed in 4% buffered formaldehyde supplemented with 20 mM $CaCl_2$ overnight at 4°C, processed for paraffin embedding, and sectioned (5 μm).

To assess glycosaminoglycans (GAGs) present in the newly synthesized ECM, deparaffinized sections were stained with Alcian Blue and van Gieson.

Immunohistochemical Analysis

Before antigen retrieval with 10 mM citrate buffer (pH 6) at 70°C, sections were deparaffinized. Sections were digested with hyaluronidase, 8.000 units/ml (Sigma–Aldrich, St. Louis, MO) in 0.1 M phosphate buffered saline (PBS) for

60 minutes at 37°C, followed by incubation with 10% goat serum (ThermoFisher, Waltham, MA) in 0.1 M PBS for 15 minutes to block nonspecific binding sites. Afterwards, sections were treated with monoclonal mouse anti-human type II collagen (Clone II-4CII; MP Biomedicals, Santa Ana, CA) for 1 hour at a 1/150 dilution. Before staining with secondary goat anti-mouse IgG conjugated with Alexa Fluor 546 (A11030; ThermoFisher, Waltham, MA), the sections were once again blocked with 10% goat serum in 0.1 M PBS for 15 minutes. After incubation for 1 hour with secondary antibody (1/300 dilution), the sections were washed in PBS. Mounting solution (ProLongGold antifade Mountant with DAPI; Thermo Fischer) was applied and the sections were stored overnight at 4°C. Positive staining for human type II collagen was confirmed with the use of native human knee cartilage. A monoclonal mouse IgG antibody (Mouse IgG1 K Isotype Control Purified; eBioscience, Thermo Fischer) was used as a negative control in a 1/75 dilution. Stained sections were analyzed using a Nikon Eclipse 90i epi-fluorescence microscope equipped with a Nikon DS-Fi2 color camera head, a DS-U3 camera controller, and a NIS-Elements imaging software suite (Version D 4.10.02; Nikon Instruments Inc, Melville, NY).

Fluorescence In Situ Hybridization

To determine whether the chondrocytes or the MSCs deposited GAG, fluorescence in situ hybridization (FISH) for human chromosomes X and Y was used. In short, sections were deparaffinized, dehydrated in EtOH series, and pretreated with sodium thiocyanate at 80°C for 30 minutes and RO-H_2O for 3 minutes. After a further protease treatment at 37°C for 45 minutes, samples were again dehydrated in EtOH series, probed with Vysis CEP X/Y (Cat # 07J22-050, Abbot Laboratories, North Chicago, IL), denatured at 85°C for 5 minutes, and hybridized overnight at 37°C. Stained sections were washed post-hybridization with SSC/0.05% Tween before counterstaining with DAPI.

Biomechanical Analysis

Mechanical properties of explants and nonimplanted scaffolds were assessed with a universal testing machine (Instron Model 5565A, Norwood, MA) equipped with a 100-N load cell, and a cylindrical plane-ended stainless steel indenter (Ø 12 mm). Unconfined compression tests were performed in wet conditions in Hanks balanced salt solution (HyClone, GE Healthcare) at room temperature. Initial dimensions of the samples were measured with a digital caliper and high-quality image analysis using the imaging software ImageJ. With increments of 10%/s, samples were compressed until 40% compressive strain. Maximum compressive stress at 40% strain was calculated for all samples, using a Bluehill software (Instron).

RESULTS

3D Bioprinting of Cell-laden Constructs

The CAD file used to control the 3D bioprinting of the constructs resulted in a good architecture of lattice-shaped constructs, suitable to provide oxygen and nutrient diffusion into the cell-laden hydrogel bioink. Cross-linking with $CaCl_2$ yielded good mechanical properties of the nanofibrillated cellulose/alginate scaffolds.

Mechanical Properties of Constructs In Vivo

All constructs showed good handling properties. Cell-laden and cell-free implants were integrated in subcutaneous tissue already after 14 days (Fig. 1). We observed an improved stiffness of the printed constructs after 60 days in vivo. All constructs remained in good shape and with preserved mechanical properties.

Neocartilage Formation In Vivo

Neocartilage formation of cell-laden NFC-A constructs was evaluated after 14, 30, and 60 days of subcutaneous implantation in nude mice. FISH and histopathological tests demonstrated human cartilage formation in the construct. GAG synthesis was examined using Alcian Blue and van Gieson staining. No positive staining was found in the cell-free scaffolds and the hBMSC samples. A gradual increase in GAG deposition was observed in both the hNC group and the coculture group, and appeared more pronounced in the hNC/hBMSC group (Fig. 2). Immunohistochemistry for human type II collagen confirmed the deposition of chondrogenic ECM after 60 days of implantation (Fig. 3). FISH for human chromosomes X and Y showed that only human nasoseptal chondrocytes had proliferated, formed cell clusters, and synthesized GAGs and type II collagen (Fig. 4). After 60 days, the formed tissue showed all the qualitative features of proper cartilage and the formation of chondrocyte cell clusters was a clear evidence of proliferation. The cells in the cell clusters contained both human chromosomes X and Y, showing that cells were of human origin.

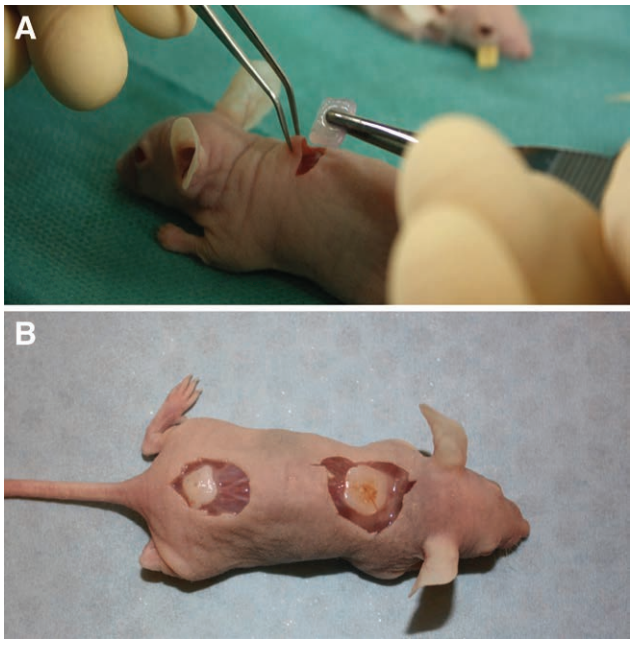

Fig. 1. Photograph of an hNC-laden scaffold after 14 days of implantation. The constructs showed good handling properties (A). The sample was surrounded by native mouse tissue and was well integrated (B).

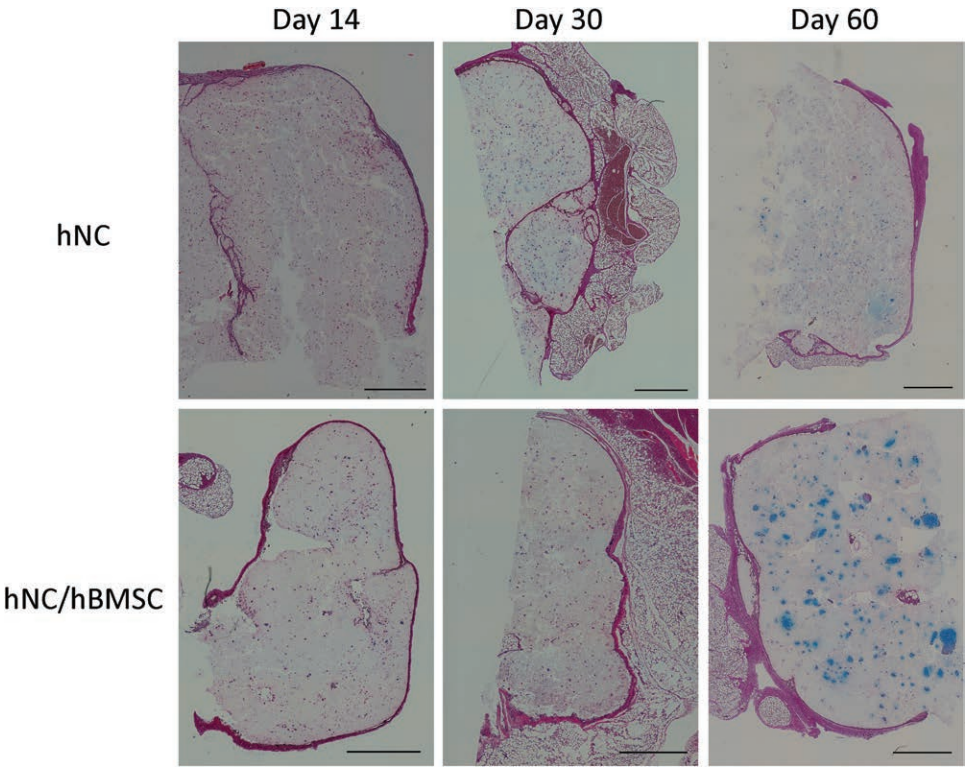

Fig. 2. Histological evaluation of GAG deposition over 60 days of implantation in hNC and hNC/hBMSC samples. Alcian Blue van Gieson staining was used to detect GAGs present in the newly synthesized ECM of day 14, day 30, and day 60 samples. Scale bars indicate 1000 μm.

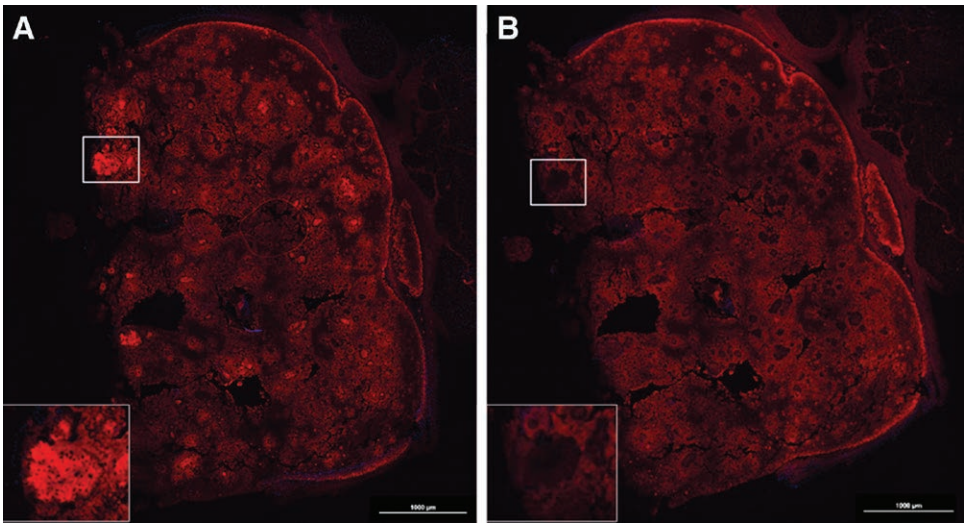

Fig. 3. Immunohistochemical analysis of hNC/hBMSC group sample after 60 days of implantation. Samples were stained with mouse antihuman type II collagen antibody (A), and mouse IgG antibody (isotype control) (B) to evaluate human type II collagen formation in the newly synthesized ECM. Scale bars indicate 1000 μm.

Biomechanical Analysis

Mechanical testing was performed to determine the influence of chondrogenesis on the stiffening of the implanted constructs. The implanted lattice-shaped structures became more stable over the duration of the experiment (Table 1). Cell-laden constructs performed better than cell-free ones.

DISCUSSION

The clinical relevance of this study consists of the evidence of new human cartilage formation in a 3D bioprinted construct using a coculture of human cells. FISH and histopathological analysis demonstrated the trophic role of MSCs on chondrocyte proliferation and matrix deposi-

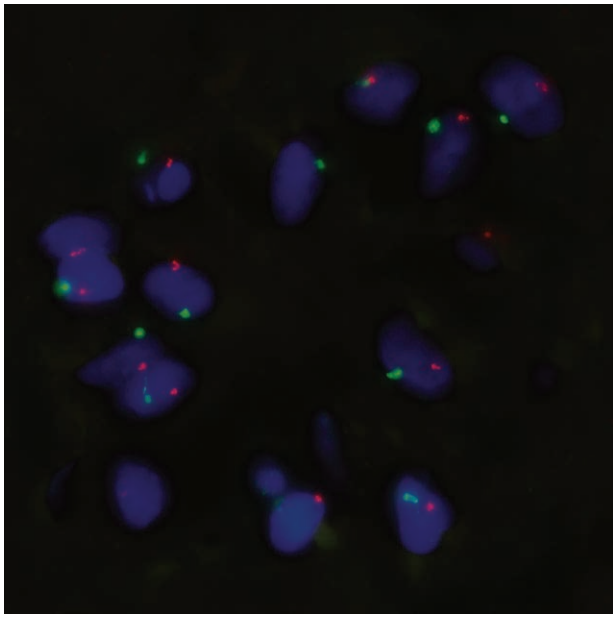

Fig. 4. FISH on a cell cluster in a coculture group sample after 60 days of implantation. Sample was probed for human chromosomes X and Y (green = Y chromosome; orange = X chromosome). Magnification ×100.

Table 1. Average Maximum Compressive Stress ± SD for Different Groups (n = 3 Per Group) at Indicated Time Points

	Maximum Compressive Stress (kPa)		
Group (3 Animals Per Group)	Day 0	Day 14	Day 60
Blank	38.9±2.5	54.0±9.8	43.0±5.4
hNC	14.9±0.8	25.8±8.1	44.0±13.4
hBMSC	14.9±0.8	35.6±1.1	88.2±15.5
hNC/hBMSC	14.9±0.8	31.4±4.9	46.0±16.8

Cell-laden constructs for day 0 were simulated by mixing growth media (DMEM/F-12) instead of cell suspension with the hydrogel. Mixing ratio (1:11) was the same as for cell-laden constructs. Blank samples were cell-free and were hydrogel alone, without media mixed in.

tion. The bioink used showed good mechanical properties and resulted a suitable environment for cell proliferation.

This study shows that the combination of nanofibrillated cellulose/alginate hydrogel, hNCs, and hBMSCs for 3D bioprinting resulted in high-fidelity constructs with good mechanical properties and a gradual increase of GAG deposition, resembling cartilage formation in vivo. As the lattice-shaped constructs were printed with space between the lines, nutrients and oxygen could diffuse through and reach the cells in the hydrogel. Such an oxygen and nutrient supply is necessary for the embedded cells to survive, proliferate, and deposit GAG. As observed for the human nasoseptal chondrocyte group and the coculture group, GAGs were formed gradually over the duration of the study. At 60 days post-implantation, a strong Alcian Blue stain surrounded the cells and showed the formation of GAG in the newly synthesized ECM. The presence of human type II collagen was confirmed by immunohistochemistry. Deposition of cartilaginous ECM appeared to be more pronounced when using a coculture of hNCs and hBMSCs, rather than a single cell type alone (Fig. 2). We used the specific 20/80 ratio as it is well established to be an optimal ratio for induction of cartilage regeneration.[22–27] The improved performance of the coculture can be attributed to a trophic role of MSCs in stimulating chondrocyte proliferation and matrix deposition. Such a beneficial role of MSCs as mediators in cartilage formation is in line with other reports demonstrating the role of trophic effects of MSCs, mediated by secreted factors and direct cell–cell contact.[23–27] It has been reported that MSCs secrete various cytokines and growth factors, which restore functions of injured tissue in vivo and enhance cell viability and proliferation in vitro.[28,29] A predominantly trophic role of the MSCs is also supported by the hBMSC group not showing any cartilaginous ECM production. It was observed that hBMSCs in the coculture group and in the hBMSC group disappeared over time. This could be due to apoptosis, which has been reported for cultured stem cells.[23] In coculture, apoptosis inducing cytokines, secreted by the chondrocytes, may have contributed to MSC death.[30] This disappearance of MSCs further points toward MSC-secreted factors being the main reason for a better performance of the coculture. Results from FISH support this trophic role of MSCs as well, rather than a chondrogenic differentiation of the MSCs (Fig. 4). The trophic effects of hMSCs have already been utilized in clinical or preclinical applications, for example, in the treatment of large-size cartilage defects or osteoarthritis.[31–33] Not only can the use of MSCs be advantageous with regard to enhancing chondrogenesis, it can also reduce the number of chondrocytes needed for treatment. As chondrocytes are a rather sparse cell type, replacing the majority of them with MSCs abundantly available in a human body (eg, in adipose tissue and bone marrow) poses a significant benefit for clinical applications. Moreover, there is no ultimate need for in vitro expansion of MSCs before application and in contrast to chondrocytes this cell type does not show dedifferentiation during in vitro cell culture.[23–25] Deposition of chondrogenic ECM is also reflected in the biomechanical analyses. In general, unconfined compression analysis showed an increase in compressive stress for cell-laden samples over the period of this pilot study. For the hNC group and the coculture group, this increase correlates with the formation and deposition of GAG and human type II collagen. However, the strong increase in maximum compressive stress for the hBMSC group at 60 days post-implantation cannot be attributed to GAG or type II collagen formation, as analysis of stained histological sections showed that there were no cells left in the bioprinted construct (data not shown). Therefore, we conclude that residual host tissue has affected the measurement.

This pilot study has certain limitations. First of all, cell density plays an important role in tissue engineering of cartilage. Puelacher et al[34] reported that the cell density should preferably be greater than 20×10^6 cells/ml, whereas at low cell densities cartilage formation would be decreased. During embryogenesis of cartilage, proliferative MSCs responsible for the formation of cartilage ECM are densely packed. For tissue engineering of car-

tilage, this early stage of tissue development should be simulated to generate functional and stable cartilage. Furthermore, a high cell density would allow for increased cell–cell contact, preventing a dedifferentiation of cells and enhance proliferation and chondrogenic ECM deposition.

Secondly, the samples measured for the unconfined compression analysis were only about one third in size of the initial construct (5×5 × 1 mm). Hence, difficulties in area determination of the measured constructs have to be taken into account. As the length and height are very important input factors for the determination of the compressive stress, a considerable error from the measurement with a simple digital caliper and the use of the imaging software ImageJ for length measurement can be suspected.

Moreover, we have not been able to correlate the mechanical properties of the neocartilage of this study with native human cartilage. However, variation of ethnicity, gender, and age has not allowed the precise determination of the mechanical properties of human nasal cartilage of the septum.[35–37]

The mechanical properties of bioengineered cartilage are determined by deposition of GAG and collagen and by the cell type used.[38] Moreover, there may still have been host tissue surrounding the samples for biomechanical analysis. This residual tissue could thus have affected the outcome, especially with regard to the hBMSC group. Notwithstanding the stated limitations, our findings support that the bioink based on nanofibrillated cellulose mixed with alginate provides a suitable environment for NCs and MSCs to synthesize neocartilage in 3D bioprinted constructs in vivo. Another important finding is that the material shows excellent structural integrity and good host tissue integration in vivo.

CONCLUSIONS

In this in vivo study, we demonstrated that 3D bioprinting technology with human cell-laden hydrogels can result in cartilage synthesis in constructs with high fidelity and good mechanical properties. This study reveals clinical relevance and suggests the potential of 3D bioprinting of human cartilage for future application in reconstructive surgery.

Matteo Amoroso, MD
University of Gothenburg
Department of Plastic Surgery
Sahlgrenska University Hospital
SE-413 45 Gothenburg, Sweden
E-mail: matteoamoroso84@hotmail.it

ACKNOWLEDGMENTS

We acknowledge the excellent technical assistance of Inger Ögärd at the Department of Clinical Chemistry and Transfusion Medicine, Institute of Cytogenetics, Sahlgrenska University Hospital, Göteborg, Sweden. We also acknowledge Västra Götaland Region for supporting 3D Bioprinting Centre, Department of Chemistry and Chemical Engineering, Chalmers University of Technology, Göteborg, Sweden.

REFERENCES

1. Lindahl A. From gristle to chondrocyte transplantation: treatment of cartilage injuries. *Philos Trans R Soc Lond B Biol Sci.* 2015;370:20140369.
2. Firmin F, Marchac A. A novel algorithm for autologous ear reconstruction. *Semin Plast Surg.* 2011;25:257–264.
3. Xu T, Binder KW, Albanna MZ, et al. Hybrid printing of mechanically and biologically improved constructs for cartilage tissue engineering applications. *Biofabrication.* 2013;5:015001.
4. Kang HW, Lee SJ, Ko IK, et al. A 3D bioprinting system to produce human-scale tissue constructs with structural integrity. *Nat Biotechnol.* 2016;34:312–319.
5. Kang HW, Yoo JJ, Atala A. Bioprinted scaffolds for cartilage tissue engineering. *Methods Mol Biol.* 2015;1340:161–169.
6. Rosen W. Computer-aided design for additive manufacturing of cellular structures. *Comput Aided Des Appl.* 2007;4:585–594.
7. Boland T, Xu T, Damon B, et al. Application of inkjet printing to tissue engineering. *Biotechnol J.* 2006;1:910–917.
8. Chung JHY, Naficy S, Yue Z, et al. Bioink properties and printability for extrusion printing living cells. *Biomater Sci* 2013;1(7):763–773.
9. Guillotin B, Guillemot, F. Cell patterning technologies for organotypic tissue fabrication. *Trends Biotechnol.* 2011;29:183–190.
10. Skardal A, Zhang J, Prestwich GD. Bioprinting vessel-like constructs using hyaluronan hydrogels crosslinked with tetrahedral polyethylene glycol tetracrylates. *Biomaterials.* 2010;31:6173–6181.
11. Lee V, Singh G, Trasatti JP, et al. Design and fabrication of human skin by three-dimensional bioprinting. *Tissue Eng Part C Methods.* 2014;20:473–484.
12. Song SJ, Choi J, Park YD, et al. A three-dimensional bioprinting system for use with a hydrogel-based biomaterial and printing parameter characterization. *Artif Organs.* 2010;34:1044–1048.
13. Almeida CR, Serra T, Oliveira MI, et al. Impact of 3-D printed PLA- and chitosan-based scaffolds on human monocyte/macrophage responses: unraveling the effect of 3-D structures on inflammation. *Acta Biomater.* 2014;10:613–622.
14. Khalil S, Sun W. Bioprinting endothelial cells with alginate for 3D tissue constructs. *J Biomech Eng.* 2009;131:111002.
15. Frampton JP, Hynd MR, Shuler ML, et al. Fabrication and optimization of alginate hydrogel constructs for use in 3D neural cell culture. *Biomed Mater.* 2011;6:015002.
16. Lee JS, Hong JM, Jung JW, et al. 3D printing of composite tissue with complex shape applied to ear regeneration. *Biofabrication.* 2014;6:024103.
17. Chung JHY, Naficy S, Yue Z, et al. Bio-ink properties and printability for extrusion printing living cells. *Biomater Sci.* 2013;1:763.
18. Markstedt K, Mantas A, Tournier I, et al. 3D bioprinting human chondrocytes with nanocellulose-alginate bioink for cartilage tissue engineering applications. *Biomacromolecules.* 2015;16:1489–1496.
19. Naumann A, Dennis JE, Aigner J, et al. Tissue engineering of autologous cartilage grafts in three-dimensional *in vitro* macroaggregate culture system. *Tissue Eng.* 2004;10:1695–1706.
20. Pleumeekers MM, Nimeskern L, Koevoet WL, et al. The *in vitro* and *in vivo* capacity of culture-expanded human cells from several sources encapsulated in alginate to form cartilage. *Eur Cell Mater.* 2014;27:264–280; discussion 278.
21. Hendriks J, Riesle J, van Blitterswijk CA. Co-culture in cartilage tissue engineering. *J Tissue Eng Regen Med.* 2007;1:170–178.
22. Martínez Ávila H, Feldmann EM, Pleumeekers MM, et al. Novel bilayer bacterial nanocellulose scaffold supports neocartilage formation *in vitro* and in vivo. *Biomaterials.* 2015;44:122–133.
23. Wu L, Leijten JC, Georgi N, et al. Trophic effects of mesenchymal stem cells increase chondrocyte proliferation and matrix formation. *Tissue Eng Part A.* 2011;17:1425–1436.

24. Zuo Q, Cui W, Liu F, et al. Co-cultivated mesenchymal stem cells support chondrocytic differentiation of articular chondrocytes. *Int Orthop.* 2013;37:747–752.
25. Wu L, Prins HJ, Helder MN, et al. Trophic effects of mesenchymal stem cells in chondrocyte co-cultures are independent of culture conditions and cell sources. *Tissue Eng Part A.* 2012;18:1542–1551.
26. de Windt TS, Hendriks JA, Zhao X, et al. Concise review: unraveling stem cell cocultures in regenerative medicine: which cell interactions steer cartilage regeneration and how? *Stem Cells Transl Med.* 2014;3:723–733.
27. Leijten JC, Georgi N, Wu L, et al. Cell sources for articular cartilage repair strategies: shifting from monocultures to cocultures. *Tissue Eng Part B Rev.* 2013;19:31–40.
28. Meirelles LS, Fontes AM, Covas DT, et al. Mechanisms involved in the therapeutic properties of mesenchymal stem cells. *Cytokine Growth Factor Rev.* 2009;20:419–427.
29. Weil BR, Markel TA, Herrmann JL, et al. Mesenchymal stem cells enhance the viability and proliferation of human fetal intestinal epithelial cells following hypoxic injury via paracrine mechanisms. *Surgery.* 2009;146:190–197.
30. Secchiero P, Melloni E, Corallini F, et al. Tumor necrosis factor-related apoptosis-inducing ligand promotes migration of human bone marrow multipotent stromal cells. *Stem Cells.* 2008;26:2955–2963.
31. Djouad F, Bouffi C, Ghannam S, et al. Mesenchymal stem cells: innovative therapeutic tools for rheumatic diseases. *Nat Rev Rheumatol.* 2009;5:392–399.
32. Savkovic V, Li H, Seon JK, et al. Mesenchymal stem cells in cartilage regeneration. *Curr Stem Cell Res Ther.* 2014;9:469–488.
33. Pleumeekers MM, Nimeskern L, Koevoet WL, et al. The *in vitro* and *in vivo* capacity of culture-expanded human cells from several sources encapsulated in alginate to form cartilage. *Eur Cell Mater.* 2014;27:264–80; discussion 278.
34. Puelacher WC, Kim SW, Vacanti JP, et al. Tissue-engineered growth of cartilage: the effect of varying the concentration of chondrocytes seeded onto synthetic polymer matrices. *Int J Oral Maxillofac Surg.* 1994;23:49–53.
35. Griffin MF, Premakumar Y, Seifalian AM, et al. Biomechanical characterisation of the human nasal cartilages; implications for tissue engineering. *J Mater Sci Mater Med.* 2016;27:11.
36. Westreich RW, Courtland HW, Nasser P, et al. Defining nasal cartilage elasticity: biomechanical testing of the tripod theory based on a cantilevered model. *Arch Facial Plast Surg.* 2007;9:264–270.
37. Richmon JD, Sage A, Wong WV, et al. Compressive biomechanical properties of human nasal septal cartilage. *Am J Rhinol.* 2006;20:496–501.
38. Zhang L, Hu J, Athanasiou KA. The role of tissue engineering in articular cartilage repair and regeneration. *Crit Rev Biomed Eng.* 2009;37:1–57.